Inorganic Chemistry

Article

pubs.acs.org/IC

Reduction of (Formazanate)boron Difluoride Provides Evidence for an *N*-Heterocyclic B(I) Carbenoid Intermediate

Mu-Chieh Chang and Edwin Otten*

Stratingh Institute for Chemistry, University of Groningen, Nijenborgh 4, 9747 AG Groningen, The Netherlands

Supporting Information

ABSTRACT: Despite the current interest in structure and reactivity of sub-valent main group compounds, neutral boron analogues of *N*-heterocyclic carbenes have been elusive due to their high reactivity. Here we provide evidence that 2-electron reduction of a (formazanate)BF_2 precursor leads to NaF elimination and formation of an *N*-heterocyclic boron carbenoid, and describe the formation of a series of unusual BN heterocycles that result from trapping of this fragment. Subsequent chemical oxidation by XeF_2 demonstrates that the trapped (formazanate)B fragment retains carbenoid character and regenerates the boron difluoride starting material in good yield. These results indicate that the formazanate ligand framework provides a unique entry into sub-valent boron chemistry.

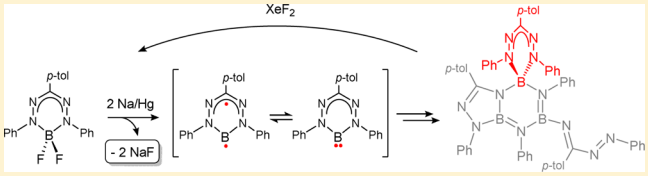

INTRODUCTION

The synthesis of reactive compounds with novel or unusual bonding motifs has fascinated chemists for centuries, and has led to new insights in the nature and stability of chemical bonds. For example, despite the (perceived) high reactivity of carbon in its divalent state, the successful stabilization of such compounds via substituent effects has led to the now ubiquitous *N*-heterocyclic carbenes (NHCs).[1] Recently, much work has focused on the synthesis of related low-valent compounds of heavier group 14 elements, which show reactivity profiles beyond those of their carbon analogues.[2] In contrast, sub-valent compounds of the group 13 elements have received considerably less attention, despite their involvement in a variety of chemical transformations. While low-valent species of the heavier group 13 elements are stabilized due to the "inert-pair" effect,[3] molecular boron(I) compounds are especially rare due to their high reactivity. Nevertheless, in the coordination sphere of transition metal centers, borylenes can be stable and show very rich coordination chemistry as well as reactivity.[4] Early work on free monomeric borylenes prepared by thermolysis of boron halides,[5] reduction of organodihaloboranes,[6] or photolysis of triarylboranes[7] showed these species to be highly reactive and to undergo C−H insertion and C═C addition reactions. More recently, matrix isolation studies have allowed spectroscopic identification of PhB,[8] and high-level theoretical calculations on the reactivity of free borylenes have been reported.[9] In the past decade, it has been shown that Lewis bases, NHCs in particular, can stabilize boron in unusual coordination environments. For example, neutral diborene[10] and diboryne[11] compounds have been prepared that are stable at room temperature. In a similar fashion, attempts to prepare base-stabilized borylenes have been reported, but these also are often still highly reactive toward C−H and C═C bonds,[12] and isolable carbene-stabilized borylenes have only been reported recently (e.g., **A** and **B** in Chart 1).[13] Attempts to obtain monomeric B(I) compounds as their *N*-heterocyclic derivatives (analogous to NHCs) have mostly been thwarted by their high reactivity, but in 2006 the group of Nozaki and co-workers described the isolation of the first nucleophilic *N*-heterocyclic boryl compound (**C**).[14] Neutral sub-valent compounds with β-diketiminate ligands have been prepared for the heavier group 13 elements (**D**),[15] but the boron analogues are unknown. The absence of isolable boron compounds of this type likely reflects the small singlet−triplet separation that is calculated to be ca. 3.5 kcal/mol.[16] Aldridge and co-workers recently described the assembly of the β-diketiminate boron fragment $HC[(CMe)(NMes)]_2B$ in the coordination sphere of an iron complex by a metal-templated approach,[17] but the direct synthesis of a neutral boron analogue of NHCs remains elusive.

Our group has been interested in the chemistry of formazanate ligands (with a NNCNN backbone) as redox-active[18] analogues of β-diketiminates (NCCCN backbone).

Chart 1

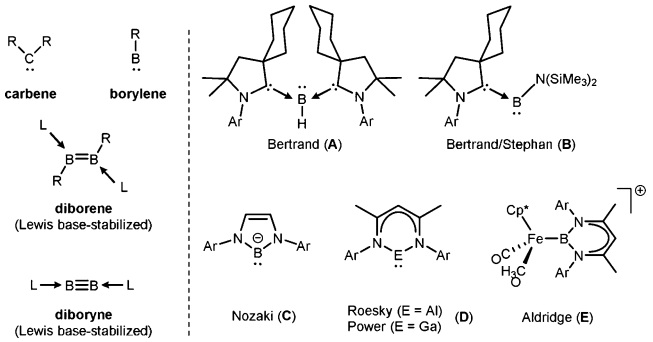

Received: June 9, 2015
Published: August 7, 2015

DOI: 10.1021/acs.inorgchem.5b01287
Inorg. Chem. 2015, 54, 8656−8664

Scheme 1. Synthesis of Compounds 3–6, with Their Constituent Fragments Shown in Brackets[a]

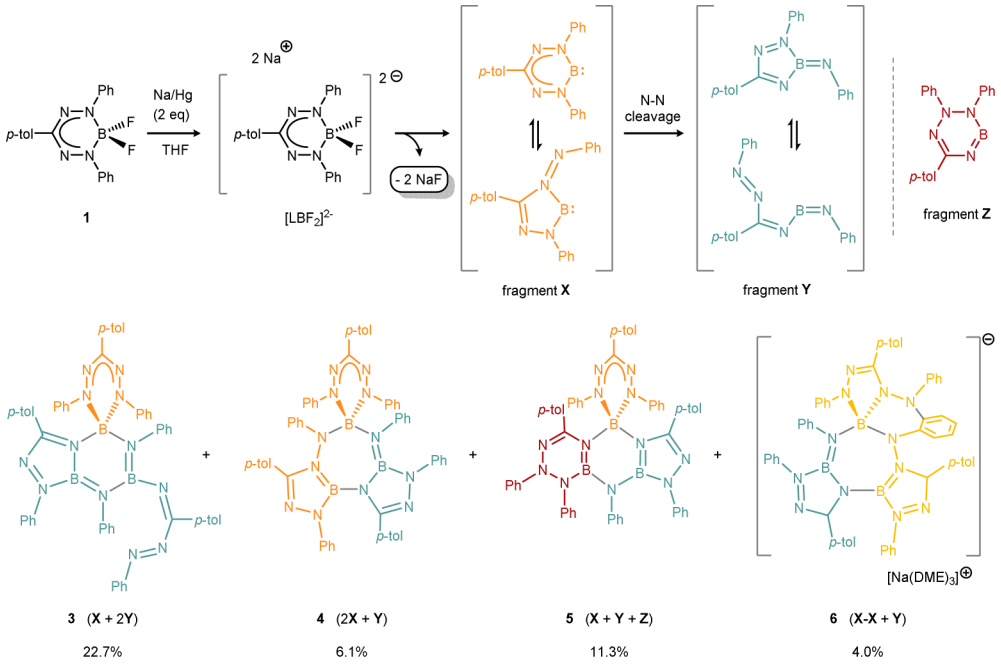

[a]The yields given correspond to isolated, crystalline material. Numbered compounds **3–6** correspond to isolated products, whereas fragments **X–Z** are putative intermediates.

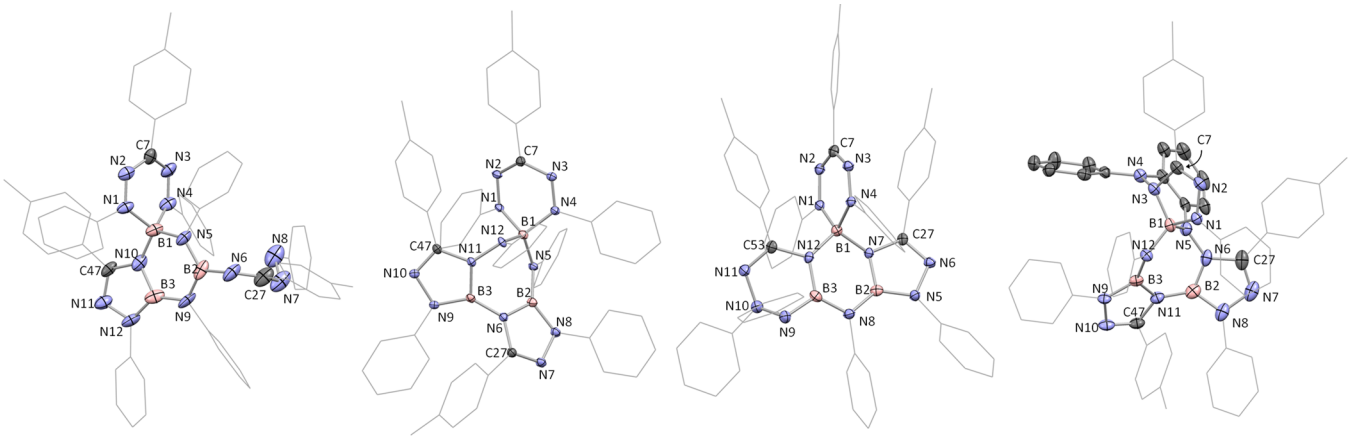

B1 – N1	1.589(9)	B1 – N1	1.614(11)
B1 – N4	1.576(9)	B1 – N4	1.539(11)
B1 – N5	1.510(8)	B1 – N5	1.522(11)
N5 – B2	1.410(9)	N5 – B2	1.441(11)
B2 – N9	1.461(9)	B2 – N6	1.451(11)
N9 – B3	1.425(9)	N6 – B3	1.444(11)
B3 – N10	1.444(9)	B3 – N11	1.411(11)
N10 – B1	1.501(8)	N11 – N12	1.411(9)
		N12 – B1	1.524(12)

B1 – N1	1.582(3)	B1 – N1	1.544(4)
B1 – N4	1.602(3)	B1 – N3	1.547(4)
B1 – N7	1.509(3)	B1 – N5	1.557(4)
N7 – B2	1.437(3)	N5 – N6	1.411(3)
B2 – N8	1.442(3)	N6 – B2	1.422(4)
N8 – B3	1.419(3)	B2 – N11	1.433(4)
B3 – N12	1.453(3)	N11 – B3	1.463(4)
N12 – B1	1.536(3)	B3 – N12	1.444(4)
		N12 – B1	1.539(4)

Figure 1. Molecular structures of compounds **3–6** (from left to right), showing 50% probability ellipsoids and selected bond distances (Å). The $Na(DME)_3^+$ counterion and hexane solvent molecule in **6**, and all hydrogen atoms are omitted; Ph and *p*-tol groups are shown as wireframe for clarity, except for the NPh groups in **6** that are coupled.

While formazanate complexes have so far received comparatively little attention, in recent years the unique properties of these ligands are becoming apparent.[19–21]

Here we report that Na/Hg reduction of a (formazanate)BF_2 compound results in a series of trimeric products that incorporate an intact *N*-heterocyclic (formazanate)B fragment, from which the starting material may be regenerated upon treatment with XeF_2. The experimental data are complemented by a computational study, which suggests involvement of a relatively stable (formazanate)B carbenoid intermediate.

RESULTS AND DISCUSSION

Reduction Chemistry. The synthesis and characterization of formazanate boron difluoride compound **1** has been described previously by us,[20b] and an improved synthesis was subsequently reported by Gilroy and co-workers.[20d] Cyclic voltammetry (CV) of **1** showed two quasi-reversible reductions

DOI: 10.1021/acs.inorgchem.5b01287
Inorg. Chem. 2015, 54, 8656–8664

at −0.98 and −2.06 V vs $Fc^{0/+}$, indicative of ligand-based redox-chemistry. Compound **1** can be converted to a green radical anion $[(PhNNC(p\text{-tolyl})NNPh)BF_2]^-$ (**2**) upon chemical reduction using Cp_2Co as the reducing agent, and the spectroscopic and structural changes accompanying this conversion indicate a "borataverdazyl"-type structure for **2**.[20a,b] Accessing the second reduction product observed by CV requires a reducing agent stronger than Cp_2Co. To explore the possibility of isolating the putative 2-electron reduction product, experiments were carried out in which **1** was reacted with 2 equiv of sodium amalgam in a THF/toluene solvent mixture, which resulted in a gradual color change from red to purple. NMR analysis of the crude reaction mixture indicated the presence of several diamagnetic products, none of which contained fluorine (on the basis of ^{19}F NMR spectroscopy). Fractional crystallization allowed the isolation and structural characterization of the four main components in the mixture, accounting in total for ca. 45% of the starting material. The major component, compound **3**, was isolated in 22.7% yield and characterized by single-crystal X-ray crystallography. The structure determination of **3** established that it contains a central B_3N_3 heterocyclic core (Scheme 1, molecular structure in Figure 1). Except for the fluorine atoms, all other atoms originally present in the boron starting material are retained in **3**: its composition suggests it is a trimer of (formazanate)-boron-derived products. On the basis of the observed atom connectivity, we propose that compound **3** is formed by assembly of the putative reduction intermediates **X** and **Y** in a 1:2 ratio. Compound **3** does not contain fluorine, suggesting that the initial 2-electron reduction product $[LBF_2]^{-2}$ is unstable in the presence of Na^+ cations (from the Na/Hg reducing agent). Although the B−F bond is among the most stable chemical bonds (B−F BDE = 732 kJ/mol,[22] calculated for BF_3 = 720−724 kJ/mol),[23] the lattice energy of NaF (910 kJ/mol)[22] provides the driving force for the loss of 2 equiv of F^- from $[LBF_2]^{2-}$ to (transiently) generate fragment **X**. Unfortunately, only alkali metal-based reducing agents are sufficiently reducing to provide access to $[LBF_2]^{2-}$.[24] It is likely that these will all result in fluoride abstraction, resulting in products that are different than $[LBF_2]^{2-}$ which is obtained by electrochemical methods. Of the fragments that constitute **3**, one contains an intact boron formazanate moiety (fragment **X**) while for the other N−N bond cleavage has occurred to give an imidoborane (fragment **Y**). The latter transformation has precedent in β-diketiminate chemistry, where reductive cleavage of the ligand backbone has been observed both in transition metal[25] and main group chemistry.[26] A second species, compound **4**, was separated from the reaction mixture in 6.1% yield as crystalline material, and this was also subjected to X-ray diffraction analysis. The molecular structure of **4** contains a central 7-membered $[B_3N_4]$ ring. Similar to **3**, compound **4** is also a heterotrimer, but it consists of two intact (formazanate)boron moieties (**X**) and one fragment (**Y**) that results from N−N bond cleavage (Scheme 1, molecular structure in Figure 1). For the intact formazanates in **4**, one is bound to the boron center via the two terminal nitrogen atoms of the NNCNN backbone while the other forms a 5-membered chelate ring in which one of the terminal nitrogen atoms is available to bridge to a second B center.

Two additional products could reproducibly be isolated by fractional crystallization. Compound **5**, which was obtained in 11.3% yield, was shown by X-ray crystallography to contain one intact (formazanate)B fragment incorporated into a B_3N_3 core that is similar to **3** (Scheme 1, molecular structure in Figure 1). However, the atom connectivity in the 6-membered chelate ring around B(3) is unexpected: it contains a NNNCN backbone in which a terminal N-Ph group has migrated onto the other N-Ph moiety of the formazanate ligand to result in a triazenyl heterocycle (fragment **Z**, *vide infra*). Finally, a fourth component (compound **6**) could be obtained from the reaction mixture in 4.0% yield and shown to be an ionic product in which the anionic part is composed of three (formazanate)-boron-derived fragments that are assembled into a 7-membered B_3N_4 core similar to **4** (Scheme 1, molecular structure in Figure 1). The countercation is Na^+, which is coordinated by three molecules of DME (the solvent of crystallization). The salient feature of **6** is the presence of a phenylene linker that connects two formazanate fragments. While the pathway to formation of the *ortho*-disubstituted C_6H_4 fragment in **6** is not known in detail, it is likely that it involves addition of a nitrogen-centered radical to the C_6H_5 ring via homolytic aromatic substitution.[27]

Due to the weak diffraction of crystals of **3** and **4**, for which only small platelets could be obtained, the crystallographic data for these compounds are of low quality. Nevertheless, the atom connectivity is clearly established, and a brief discussion of the metrical parameters is included below. The crystal structures of **3**−**5** show similar metrical parameters for the intact 6-membered formazanate chelate ring. The N−N bond distances vary little (**3**, 1.317(6)/1.316(6) Å; **4**, 1.302(8)/1.322(8) Å; **5**, 1.308(2)/1.298(2) Å) and are similar to the values found in the starting material **1** (1.3080(13)/1.3078(13) Å). This indicates that the formazanate is retained as a delocalized monoanionic ligand (L^-), with little or no contribution from the radical dianionic form (L^{2-}) that we characterized recently.[20b,21a,b] The B(1) boron atom in compounds **3**−**6** is tetracoordinate, while the boron centers B(2) and B(3) are tricoordinate. Of the 4 B−N bonds around the tetracoordinate B(1) atom in compound **3**, those to the nitrogen atoms in the central B_3N_3 ring are the shortest (B(1)−N(5) = 1.510(8) Å and B(1)−N(10) = 1.501(8) Å), but still significantly elongated in comparison to those for the tricoordinate B atoms (B−N distances 1.409(8)−1.460(9) Å). Similar values are found for the other compounds. The B_3N_3 core in **3** is somewhat reminiscent of borazine $(HN{=}BH)_3$, often referred to as the inorganic analogue of benzene,[28] but in contrast to **3**, borazine shows equivalent (delocalized) B−N bonds of 1.430 Å.[28a] While recent calculations on donor/acceptor complexes of borazine and its derivatives suggested that binding of an external Lewis base (NH_3) is not energetically favorable,[29] the presence of 4-coordinate boron atoms around the B_3N_3 core in **3** and **5** suggests these to have significant acceptor properties. The metrical parameters for the B_3N_3 core in **5** are similar to those in **3**, and both are virtually planar. In addition to the central B_3N_3 ring, compound **5** contains a highly puckered BNNNCN 6-membered heterocycle in which the triazenyl chain shows long consecutive N−N bonds in the N(9)−N(10)−N(11) fragment of 1.413(2) and 1.403(2) Å. A similarly long N−N bond is found in the puckered B_3N_4 core of **4** (N(11)−N(12) = 1.411(9) Å). These N−N bonds are significantly elongated in comparison to those in delocalized formazanate ligands and are indicative of N−N single bond character. The $[B_3N_4]$ core in **6** is similar to that in **4** with both compounds adopting a pseudo-boat conformation of the 7-membered heterocycle. Although compounds **3**−**6** are diamagnetic, their NMR spectra are not very informative. The ^1H NMR spectra contain several overlapping sets of resonances in the aromatic region. More

DOI: 10.1021/acs.inorgchem.5b01287
Inorg. Chem. 2015, 54, 8656−8664

diagnostic is the aliphatic region: as expected, each compound shows three separate singlets in the range of δ 2.0−2.5 ppm, consistent with three different *p*-tolyl CH_3 environments as required for the C_1 symmetric trimers observed in the solid state. Furthermore, the ^{11}B NMR spectrum for each compound shows two resonances: a broad signal around δ 26 ppm (fwhh > 700 Hz) and a somewhat sharper one around δ 0 ppm (fwhh < 220 Hz) that are attributed to the 3- and 4-coordinate B centers, respectively.

UV−vis spectroscopy for **3**−**5** in THF solution (Figure 2) shows broad absorption features in the visible range of the

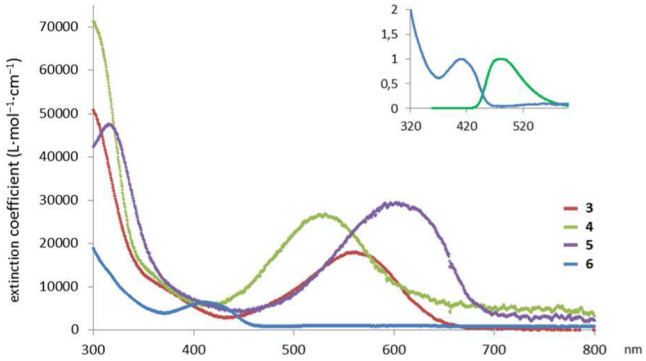

Figure 2. UV−vis spectra for compounds **3**−**6** in THF solution. Inset: Emission spectrum of **6** showing normalized intensities.

spectrum that account for their intense color (ε = 19000−30000 $L{\cdot}mol^{-1}{\cdot}cm^{-1}$). Compound **3** has a maximum absorption at 557 nm that is due to the formazanate $\pi-\pi^*$ transition,[20c,30] similar to that observed in **1** (λ_{max} = 521 nm).[20b] Compounds **4** and **5** show absorption maxima at lower and higher wavelengths (527 and 601 nm, respectively). Conversely, the appearance of the spectrum of **6** is quite different with a much less intense absorption at λ_{max} = 408 nm (ε = 6400 $L{\cdot}mol^{-1}{\cdot}cm^{-1}$). The difference between **3**−**5** and **6** is due to the absence of a delocalized 6-membered formazanate [NNCNN] chelate ring in **6**. Formazanate boron difluorides have recently been investigated as analogues of BODIPY dyes and showed tunable luminescence properties, with quantum yields of up to 77% for compounds with a 3-cyanoformazanate ligand.[20c,d] We thus investigated the emission spectra of **3**−**6** in THF solution. Whereas the neutral compounds **3**−**5** are only weakly emissive, compound **6** shows a relatively intense emission band at 477 nm (Stokes shift of 69 nm) upon excitation at 400 nm with a quantum yield of 6%.

Density Functional Theory (DFT) Calculations. While it proved not possible to obtain experimental evidence for the existence of fragment **X** as an intermediate, we probed the pathway that leads to compounds **3**−**5** by DFT calculations at the B3LYP/6-31G(d) level in the gas phase. For these calculations, the *p*-tolyl group in **3**−**5** was replaced by Ph for computational efficiency. We first evaluated the relative stabilities of the possible intermediates **X** and **Y** and compared those to the isolated products. The two-electron reduction of **1** was observed by cyclic voltammetry to occur at $E_{1/2}$ = −2.06 V vs $Fc^{0/+}$ to form the dianionic species $[LBF_2]^{2-}$.[20b] In the presence of Na^+ this is thought to be unstable toward elimination of NaF (2 equiv), which would lead to the suggested carbenoid intermediate **X**. The geometry of **X** was optimized in the gas phase in the closed-shell singlet ($\mathbf{X_s}$), triplet ($\mathbf{X_t}$), and singlet diradical states ($\mathbf{X_{BS}}$). The optimized geometry on the singlet potential energy surface shows a puckered formazanate boron chelate ring for $\mathbf{X_s}$, which is calculated to be higher in energy than the triplet $\mathbf{X_t}$ (ΔG = 6.8 kcal/mol). A broken-symmetry, singlet diradical solution ($\mathbf{X_{BS}}$) is shown to be slightly higher in energy than the triplet. Thus, these calculations indicate that the ground state for **X** contains a ligand-based unpaired electron spin which is ferromagnetically coupled to a boron-based unpaired electron (J_{calcd} = −40.8 cm^{-1}). The ground-state structure $\mathbf{X_t}$ is virtually planar and shows elongated N−N bonds of 1.380 Å, indicative of population of the N−N π^* orbitals and the presence of a reduced "verdazyl"-type radical dianionic ligand ($L^{\bullet 2-}$).[20b] Thus, the ground-state electronic structure of **X** is different than that of a borylene, with the unpaired electrons in **X** occupying an sp^2 orbital on B and a ligand-based π^* orbital which leads to a (triplet) diradical ground state (Figure 3). This

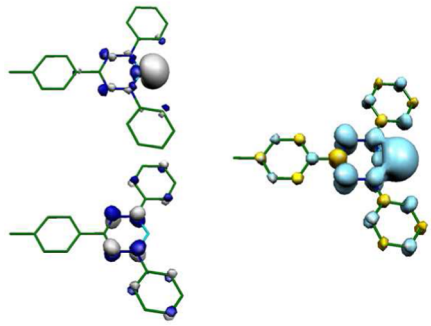

Figure 3. Singly occupied frontier molecular orbitals (left) and spin density plot (right) for the ground-state triplet $\mathbf{X_t}$.

is in agreement with calculations on related boron compounds.[16,31] While the small singlet−triplet gap in neutral *N*-heterocyclic boron(I) compounds is suggested as the reason for their high reactivity (and absence from the literature),[16b] our results indicate that the increased stability for the biradical state due to the low-lying formazanate π^*-orbital can in fact be used advantageously to allow isolation of several trapped (formazanate)B species.

The (singlet) imidoborane fragment **Y** was also computationally evaluated and shown to be significantly more stable than $\mathbf{X_s}$ with ΔG = −51.42 kcal/mol for the *Z*-isomer (which is incorporated into the isolated products). Fragment **Z**, which is one of the constituents in trimer **5** is shown to have a singlet ground state that is slightly more stable than $\mathbf{X_s}$ (ΔG = −5.39 kcal/mol).

Geometry optimizations of the final products **3**, **4**, and **5** converged on minima ($\mathbf{3_{calc}}$−$\mathbf{5_{calc}}$) that are in good agreement with the experimentally determined structures. Specifically, the characteristic N−N bonds in the 6-membered formazanate chelate rings range between 1.296 and 1.304 Å in the DFT models, and the metrical parameters of the central B_3N_3 and B_3N_4 heterocycles are reproduced accurately. Formation of the experimentally observed products is calculated to be very exergonic from the respective fragments, with ΔG = −118.4, −163.4, and −155.7 kcal/mol for $\mathbf{3_{calc}}$, $\mathbf{4_{calc}}$, and $\mathbf{5_{calc}}$, respectively (all energies relative to the fragments $\mathbf{X_s}$, *E*-**Y**, and **Z**; see Supporting Information for details).

Reduction Chemistry. The BN-heterocycles **3**−**6** contain an intact formazanate unit that can be expected to show (reversible) redox-chemistry that is typical of the formazanate NNCNN ligand backbone. To test this hypothesis, cyclic

DOI: 10.1021/acs.inorgchem.5b01287
Inorg. Chem. 2015, 54, 8656−8664

voltammetry was recorded in THF solution using $[Bu_4N][PF_6]$ as the supporting electrolyte. The data for **3** show a complicated electrochemical response, analysis of which is beyond the scope of the present paper (see Figure S1). Conversely, compounds **4** and **5** show quasi-reversible, sequential 1-electron redox processes (Figure 4) that are

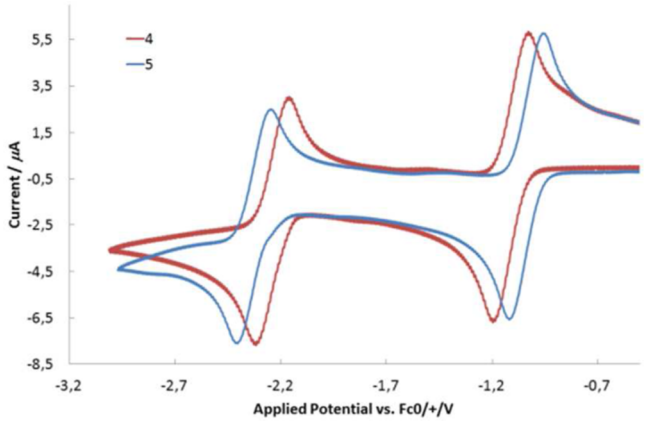

Figure 4. Cyclic voltammograms of **4** and **5** in THF (0.1 M $[Bu_4N][PF_6]$) recorded at 100 mV·s^{-1} (potential in V vs $Fc^{0/+}$).

reminiscent of those observed for **1**. These correspond to the reversible formation of the radical anions of $\mathbf{4}^{\bullet-}$ or $\mathbf{5}^{\bullet-}$ (−1.13 and −1.06 V vs $Fc^{0/+}$) and the corresponding dianions ($\mathbf{4}^{2-}$ or $\mathbf{5}^{2-}$, −2.26 and −2.35 V vs $Fc^{0/+}$), respectively. The first reduction occurs at more negative potential than that in the boron difluoride starting material **1** (−0.98 V vs $Fc^{0/+}$),[20b] and is only marginally easier for **5** than for **4**. For the second reduction to $\mathbf{4}^{2-}$ and $\mathbf{5}^{2-}$ the order is reversed, and $\mathbf{4}^{2-}$ is formed at a potential ca. 0.09 V less negative than $\mathbf{5}^{2-}$.

Although the cyclic voltammetry data suggest that the radical anion $\mathbf{3}^{\bullet-}$ might not be stable, we nevertheless attempted its synthesis. Chemical reduction of compound **3** was carried out in THF solution using a stoichiometric amount of Na/Hg, which resulted in a color change to very dark green. Upon diffusion of hexane into the THF solution, a black powder is precipitated together with a small amount of green crystalline material. X-ray analysis of the crystals confirmed it to be the expected reduction product $[Na(THF)_3]^+[\ \mathbf{3}]^{\bullet-}$. Unfortunately, the desired product was always obtained together with the (unidentified) black powder, and an analytically pure sample has not been obtained.

The X-ray structure determination shows that a Na^+ countercation (with three coordinated THF molecules) is bound to N(11) of the BNNCN 5-membered ring of $\mathbf{3}^{\bullet-}$ (Figure 5). The radical anion $\mathbf{3}^{\bullet-}$ is virtually isostructural to the neutral precursor **3**, but the N−N bonds within the intact formazanate NNCNN fragment are elongated significantly ($\mathbf{3}^{\bullet-}$, 1.359(4)/1.355(4) Å; **3**, 1.317(6)/1.316(6) Å), as expected for a formazanate-based reduction.

Similarly, the reduction of **5** with Na/Hg in THF solution resulted in a color change to deep green, and the radical anion $\mathbf{5}^{\bullet-}$ was obtained as its Na^+ salt in quantitative yield by recrystallization in the presence of 15-crown-5. The structure determination shows two $\mathbf{5}^{\bullet-}$ fragments, one of which contains a Na^+(15-crown-5) cation bound to a triazenyl N atom (Figure 5). A second Na^+(15-crown-5) bridges between the two $\mathbf{5}^{\bullet-}$ units via the BNNCN 5-membered rings (full structure shown in Figure S2). The metrical parameters for the two independent

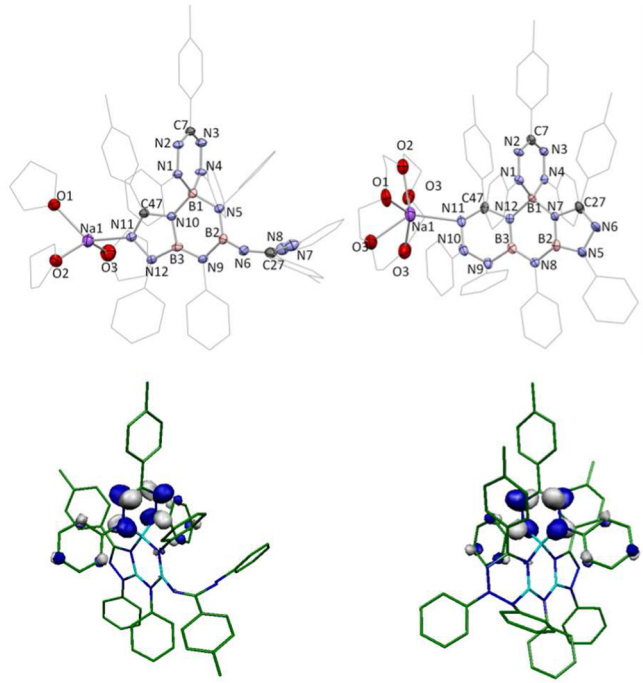

Figure 5. Molecular structures of compounds $[Na(THF)_3]^+[\mathbf{3}]^{\bullet-}$ (top left) and $[Na(15\text{-c-}5)]^+[\mathbf{5}]^{\bullet-}$ (one of the independent molecules, top right) showing 50% probability ellipsoids. The Ph/*p*-tol groups and the C atoms of the THF/15-crown-5 molecules are shown as wireframe for clarity. DFT models of $[\mathbf{3}]^{\bullet-}$ (bottom left) and $[\mathbf{5}]^{\bullet-}$ (bottom right) showing the SOMO.

$[\mathbf{5}]^{\bullet-}$ moieties are very similar, and only one of them will be discussed. Although the quality of the structure determination of $[Na(15\text{-c-}5)]^+[\mathbf{5}]^{\bullet-}$ is negatively affected by the disorder observed in the bridging Na^+(15-crown-5), it is clear that the integrity of the BN-heterocycle **5** is retained upon reduction to the radical anion $\mathbf{5}^{\bullet-}$. The formazanate N−N bond lengths range between 1.355(4) and 1.362(4) Å, indicating that the formazanate ligand backbone is the electron acceptor. In addition, the B−N(formazanate) bonds around the 4-coordinate B center are contracted from 1.582(3)/1.602(3) Å in **5** to 1.538(5)/1.540(5) Å in $\mathbf{5}^{\bullet-}$, with concomitant elongation of the B−N bonds to the central 6-membered heterocyclic ring (B(1)−N(7)/B(1)−N(12) in **5**, 1.509(3)/1.536(3) Å, and $\mathbf{5}^{\bullet-}$, 1.537(5)/1.598(5) Å).

Geometry optimizations of the radical anions $[\mathbf{3}]^{\bullet-}$ and $[\mathbf{5}]^{\bullet-}$ (gas-phase calculations in the absence of the Na^+ countercation) at the UB3LYP/6-31G(d) level of theory converged on minima that have very similar metrical parameters as the crystallographically determined structures. In agreement with the experimental data, the SOMO in both radical anions is localized on the formazanate backbone and has N−N antibonding character.

Chemical Oxidation. In attempts to elicit reactivity that stems from the trapped (formazanate)B carbenoid fragment, we treated compounds **3**−**5** with the oxidizing agent XeF_2. The reaction between **3** and XeF_2 was monitored in an NMR tube (C_6D_6 solution). Addition of 1 or 2 equiv of XeF_2 relative to **3** (XeF_2:B ratio < 1) resulted in rapid disappearance of the starting material, but an intractable mixture was obtained.

Surprisingly, reaction with 3 equiv of XeF_2 resulted in a signal in the ^{19}F NMR spectrum that is diagnostic for the boron difluoride starting material (PhNNC(*p*-tolyl)NNPh)BF_2 (**1**).

DOI: 10.1021/acs.inorgchem.5b01287
Inorg. Chem. 2015, 54, 8656−8664

Addition of a larger excess of XeF_2 to **3** (12 equiv, XeF_2:B ratio = 4) converted 90% of the (formazanate)B fragment **X** present in **3** to the difluoride **1** after 30 min, with quantitative conversion after standing overnight (based on ^{19}F NMR integration relative to an internal standard). As may be anticipated, only the moiety with the intact NNCNN formazanate backbone (indicated in bold in Scheme 2) is

Scheme 2. Chemical Oxidation of Compounds 3 and 4 To Regenerate the Boron Difluoride 1[a]

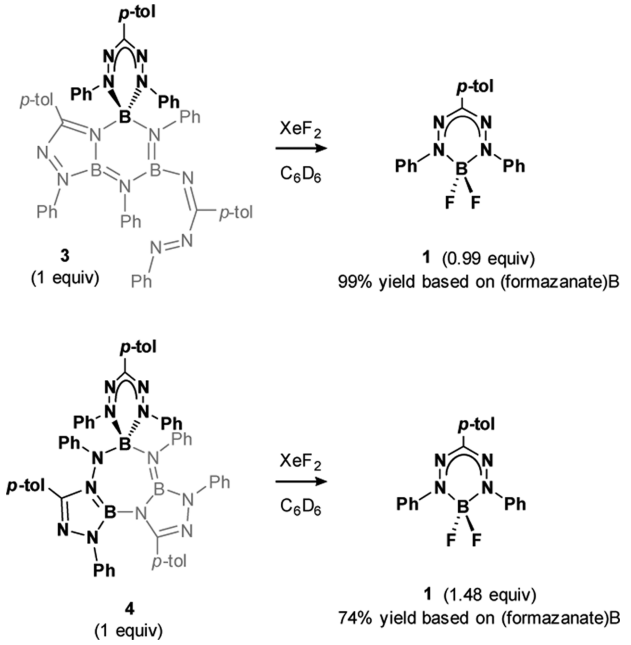

[a]Yields are based on the amount of (formazanate)B available in the starting material (indicated in bold).

able to regenerate **1**. The fate of the remaining B-containing fragments is unclear at present. While we were unable to observe similar reactivity between **5** and XeF_2 (3 or 12 equiv), also **4** reacted with excess XeF_2 to give the boron difluoride **1** (Scheme 2). Compound **4** contains two intact (formazanate)B fragments (**X**, as 5- and 6-membered chelates) which are both converted to **1**, leading to a total of 1.48 equiv (74% yield based on available (formazanate)B) after 16 h.

It is at present unclear why compounds **3** and **4** give good yields of **1** upon oxidation with XeF_2, but **5** does not. Also, the mechanism for the reaction with XeF_2 is not known and needs further investigation. Nevertheless, these results demonstrate that the "trapped" (formazanate)B species is able to show carbenoid reactivity at the boron center. [31b]

CONCLUSIONS

Although the high reactivity of triplet boron carbenoids has been suggested as the reason for their conspicuous absence from the literature, our results indicate that judicious ligand design imparts sufficient stability to allow isolation of novel BN-heterocycles derived from the carbenoid fragment (PhNNC(*p*-tolyl)NNPh)B (**X**). Fragment **X** is calculated to have a triplet biradical ground state that is stabilized due to the low-lying formazanate π^*-orbitals. Reductive cleavage of a N−N bond in **X** generates the iminoborane species **Y**, and these two intermediates combine under the reaction conditions to form the final trimeric products. The (formazanate)B fragment that is incorporated in the BN-heterocyclic products **3**−**6** remains available as a redox-active moiety, as shown by cyclic voltammetry and X-ray structural characterization of the radical anions $[\mathbf{3}]^{\bullet-}$ and $[\mathbf{5}]^{\bullet-}$. Significantly, the (formazanate)B moiety retains carbenoid character and is able to perform a net 2-electron oxidative addition reaction with XeF_2 that regenerates the boron difluoride starting material **1**. The results presented here highlight that formazanate ligands have considerable potential in stabilizing highly reactive B compounds, and demonstrate a novel design strategy toward the synthesis of isolable *N*-heterocyclic boron carbenoids.

EXPERIMENTAL SECTION

General Considerations. All manipulations were carried out under nitrogen atmosphere using standard glovebox, Schlenk, and vacuum-line techniques. Toluene, hexane, and pentane (Aldrich, anhydrous, 99.8%) were passed over columns of Al_2O_3 (Fluka), BASF R3-11-supported Cu oxygen scavenger, and molecular sieves (Aldrich, 4 Å). Diethyl ether and THF (Aldrich, anhydrous, 99.8%) were dried by percolation over columns of Al_2O_3 (Fluka). Deuterated solvents were vacuum transferred from Na/K alloy (C_6D_6, THF-d_8, Aldrich) or CaH_2 (CD_2Cl_2) and stored under nitrogen. XeF_2 was purchased from Alfa Aesar and used as received. The compound [PhNNC(*p*-tolyl)NNPh]BF_2 (**1**) was synthesized according to a published procedure.[20b] NMR spectra were recorded on Varian Gemini 200, VXR 300, Mercury 400, Inova 500, or Agilent 400 MR spectrometers. The ^1H and ^{13}C NMR spectra were referenced internally using the residual solvent resonances and reported in ppm relative to TMS (0 ppm); *J* is reported in Hz. Assignment of NMR resonances was aided by gradient-selected gCOSY, NOESY, gHSQCAD and/or gHMBCAD experiments using standard pulse sequences. ^{11}B NMR spectra were recorded in quartz NMR tubes using a OneNMR probe on an Agilent 400 MR system. UV−vis spectra were recorded in THF solution (~10^{-5} M) using an Avantes AvaSpec 3648 spectrometer and an AvaLight-DHS light source inside a N_2 atmosphere glovebox. The photoluminescence quantum yield of **6** was determined using an optically dilute solution in THF (λ_{ex} = 400 nm) with optically dilute fluorescein (0.5 M NaOH) as reference. Spectra were recorded using a 75 W xenon lamp coupled to a Zolix 150 monochromator coupled directly to a Qpod cuvette holder (Quantum Northwest), and emission was collected through a fiber optic connected Shamrock 163 spectrograph and iDUS-420A-OE CCD detector. Spectra are uncorrected for instrument response. Elemental analyses were performed at the Microanalytical Department of the University of Groningen or Kolbe Microanalytical Laboratory (Mülheim an der Ruhr, Germany).

Computational Studies. Calculations were performed with the Gaussian09 program using density functional theory (DFT).[32] In order to increase computational efficiency, the *p*-tolyl group was replaced by Ph. Geometries were fully optimized starting from the X-ray structures using the B3LYP exchange-correlation functional with the 6-31G(d) basis set. Geometry optimizations were performed without (symmetry) constraints, and the resulting structures were confirmed to be minima on the potential energy surface by frequency calculations (number of imaginary frequencies = 0). Transition-state calculations were performed with the QST3 algorithm in Gaussian09. The calculated transition states were confirmed by frequency calculations, which shows one imaginary frequency, and IRC calculations in both directions.

X-ray Crystallography. Suitable crystals of **3**−**6** were mounted on a cryo-loop in a drybox and transferred, using inert-atmosphere handling techniques, into the cold nitrogen stream of a Bruker D8 Venture diffractometer. The final unit cell was obtained from the xyz centroids of 9250 (**3**), 6880 (**4**), 9937 (**5**), and 9958 (**6**) reflections after integration. Intensity data were corrected for Lorentz and polarization effects, scale variation, and decay and absorption: a multiscan absorption correction was applied, based on the intensities of symmetry-related reflections measured at different angular settings

DOI: 10.1021/acs.inorgchem.5b01287
Inorg. Chem. 2015, 54, 8656−8664

Table 1. Crystallographic Data for 3−6

	3	4	5	6
chem formula	$C_{60}H_{51}B_3N_{12}$	$C_{60}H_{51}B_3N_{12}$	$C_{60}H_{51}B_3N_{12}$	$C_{75}H_{87}B_3N_{12}NaO_6$
M_r	972.55	972.55	972.55	1307.98
cryst syst	monoclinic	orthorhombic	monoclinic	monoclinic
color, habit	red, platelet	purple, platelet	purple, platelet	yellow, block
size (mm)	0.24 × 0.13 × 0.02	0.12 × 0.07 × 0.01	0.28 × 0.06 × 0.02	0.20 × 0.07 × 0.04
space group	$C2/c$	$P2_12_12_1$	$P2_1/n$	$P2_1/n$
a (Å)	32.1139(13)	11.0453(10)	10.5968(4)	13.1785(6)
b (Å)	14.4081(7)	19.3899(17)	17.7087(7)	21.1594(9)
c (Å)	25.2549(10)	22.940(2)	30.8111(10)	26.1619(10)
β (deg)	109.612(2)	99.332(2)	94.1169(13)	
V (Å^3)	11007.5(8)	4913.1(8)	5705.4(4)	7276.4(5)
Z	8	4	4	4
ρ_{calc} (g·cm^{-3})	1.174	1.315	1.132	1.194
μ(Cu Kα) (mm^{-1})	0.554	0.621	0.535	
μ(Mo Kα) (mm^{-1})				0.082
F(000)	4080	2040	2040	2780
temp (K)	100(2)	100(2)	100(2)	100(2)
θ range (deg)	3.397−56.447	2.984−54.597	2.888−65.282	2.899- 24.756
data collected (h,k,l)	−34:34, −14:16, −28:27	−11:10, −15:20, −23:23	−12:12, −20:18, −36:36	−15:15, −24:24, −30:30
min, max transm	0.917, 0.989	0.949, 0.994	0.962, 0.995	0.993, 0.997
rflns collected	50 659	24 631	55 095	94 891
indpndt reflns	7272	5883	9693	12 418
observed reflns $F_o \geq 2.0\sigma(F_o)$	4069	4522	6687	7523
$R(F)$ (%)	9.89	7.34	5.12	6.12
w$R(F^2)$ (%)	26.49	12.51	12.05	13.98
GooF	1.036	1.120	1.007	1.023
weighting a, b	0.1031, 72.3279	0, 11.9205	0.0512, 2.6001	0.0442, 6.4770
params refined	679	680	679	915
min, max resid dens	−0.286, 0.457	−0.340, 0.321	−0.223, 0.401	−0.373, 0.400

(SADABS).[33] The structures were solved by direct methods using the program SHELXS.[34] The hydrogen atoms were generated by geometrical considerations, constrained to idealized geometries, and allowed to ride on their carrier atoms with an isotropic displacement parameter related to the equivalent displacement parameter of their carrier atoms. Structure refinement was performed with the program package SHELXL.[34] Crystal data and details on data collection and refinement are presented in Table 1.

For compound **3**, several small crystals were tested, but all showed only weak diffraction images even when using a Cu microfocus source. Ultimately, a crystal was found that gave a reasonable (albeit weak) diffraction pattern, and a full data set was collected. Due to the low scattering power of the crystal, only data up to a resolution of 0.925 Å were included in the refinement. From the refinement it was clear that a highly disordered solvent molecule (most likely hexane) was present in the crystal lattice. The PLATON/SQUEEZE routine was used to remove its contribution. For compound **4**, only thin platelets could be obtained that showed weak diffraction images. A full data set was collected up to a resolution of 0.946 Å. Refinement of the structure resulted in unrealistic displacement parameters for some of the atoms, and DELU/SIMU instructions were applied in the final refinement stage. For compound **5**, a toluene solvate molecule was found to be disordered, and its contribution was removed by SQUEEZE routine implemented in PLATON. For compound **6**, refinement was frustrated by a disorder problem. From the solution it was clear that one of the Ph groups was disordered: the electron density of the atoms appeared to be spread out. The disordered Ph group was described by a two site occupancy model with separately refined displacement parameters. The s.o.f. of the major fraction refined to 0.74. DFIX and ISOR instructions were applied to restrain the N−C(Ph) bond distances to chemically reasonable values and prevent non-positive definite displacement parameters in the disordered part of the molecule.

Synthesis and Isolation of Compounds 3−6. The following procedure is representative for the synthesis and sequential isolation of pure samples of **3**−**6**:

A flask was charged with [PhNNC(*p*-tolyl)NNPh]BF_2 (**1**, 300 mg, 0.828 mmol), Na/Hg (2.447%, 1.558 g, 1.657 mmol of Na), THF (5 mL), and toluene (10 mL). The reaction mixture was stirred at room temperature for 3 days, and the color changed from red to purple. After removal of all the volatiles under vacuum, the crude reaction mixture was analyzed by ^{1}H NMR spectroscopy in C_6D_6 and shown to contain compounds **3**, **4**, and **5** in a 1:0.6:0.5 ratio based on the integration of the *p*-tolyl CH_3 resonances and comparison to isolated, pure materials (see below).

For further workup, the crude product was dissolved in dimethoxyethane (4 mL).

Isolation of 6. Slow diffusion of hexane into the dimethoxyethane solution −30 °C precipitated compound **6**. Analytically pure material was obtained by dissolving the precipitate again in dimethoxyethane, followed by diffusion of hexane into the solution to yield 14.8 mg of **6** as light yellow crysalline material (0.014 mmol, 4.0%).

Isolation of 3. Upon separation of **6**, the supernatant was pumped to dryness, and the solid residue was dissolved in a toluene/THF mixture (ratio 1:2, total 4 mL). Hexane was allowed to diffuse into the solution at −30 °C, which resulted in the precipitation of 61.8 mg of **3** as dark purple crystalline material (0.064 mmol, 22.7%).

Isolation of 5. All volatiles were removed from the supernatant that was left upon isolation of **3**. Dissolving the residue in toluene (4 mL) and allowing diffusion of hexane into the toluene layer at −30 °C afforded 33.0 mg of **5** as deep blue crystals (0.031 mmol, 11.3%).

Isolation of 4. Further concentration of the supernatant and cooling to −30 °C precipitated 16.5 mg of **4** as deep red crystalline material (0.017 mmol, 6.1%).

Characterization Data for Compound 3. ^{1}H NMR (CD_2Cl_2, 400 MHz, 25 °C): 8.03 (d, 2H, J = 8.6 Hz, *p*-tolyl CH), 7.76 (dm, 2H, J = 8.4 Hz, *p*-tolyl CH), 7.58−7.43 (m, 7H), 7.46 (t, 1H, J = 7.2 Hz,

DOI: 10.1021/acs.inorgchem.5b01287
Inorg. Chem. 2015, 54, 8656−8664

Ph *p*-CH), 7.39 (d, 2H, *J* = 8.0 Hz), 7.35 (d, 2H, *J* = 8.0 Hz), 7.22 (t, 1H, *J* = 7.4 Hz, Ph *p*-CH), 7.08−7.03 (m, 9H), 6.93 (t, 2H, *J* = 7.6 Hz, Ph *m*-CH), 6.89−6.77 (m, 11H), 6.63 (t, 1H, *J* = 7.2 Hz, Ph *p*-CH), 6.41 (d, 2H, *J* = 8.4 Hz, Ph *o*-CH), 2.32 (s, 3H, *p*-tolyl CH_3), 2.28 (s, 3H, *p*-tolyl CH_3), 2.18 (s, 3H, *p*-tolyl CH_3). ^{13}C NMR (CD_2Cl_2, 100 MHz, 25 °C): 158.1 (NCN), 152.8 (NCN), 150.8 (NCN), 147.5, 147.0, 146.7, 146.1, 144.8, 143.5, 141.7 (*p*-tolyl *p*-C), 138.4 (*p*-tolyl *p*-C), 138.3 (*p*-tolyl *p*-C), 132.7, 132.6, 132.1, 129.7, 129.6, 129.5, 129.4, 129.2, 129.1, 129.0, 128.9, 128.7, 128.5, 128.4, 128.3, 127.8, 127.8, 124.6 (*p*-tolyl CH), 124.2, 124.2 (Ph *p*-CH), 123.8 (*p*-tolyl CH), 123.5, 123.4, 21.6 (*p*-tolyl CH_3), 21.3 (*p*-tolyl CH_3), 21.2 (*p*-tolyl CH_3). ^{11}B NMR (C_6D_6, 128 MHz, 25 °C): 26.2 (fwhh = 1050 Hz), 0.5 (fwhh = 220 Hz). Anal. Calcd for $C_{60}H_{51}B_3N_{12}(C_6H_{14})_{0.5}$: C, 74.50; H, 5.76; N, 16.55. Found: C, 74.42; H, 5.49; N, 16.94.

Characterization Data for Compound 4. ^1H NMR (CD_2Cl_2, 400 MHz, 25 °C): 7.83 (d, 2H, *J* = 8.4 Hz, *p*-tolyl *o*-CH), 7.67 (d, 2H, *J* = 8.0 Hz, *p*-tolyl *o*-CH), 7.62−7.59 (m, 2H), 7.33 (d, 2H, *J* = 8.0 Hz, *p*-tolyl *m*-CH), 7.22 (d, 2H, *J* = 8.0 Hz, Ph *o*-CH), 7.14−7.10 (m, 9H), 7.05 (d, 2H, *J* = 8.4 Hz, *p*-tolyl *o*-CH), 7.00−6.87 (m, 3H), 6.97 (d, 2H, *J* = 8.0 Hz, *p*-tolyl *m*-CH), 6.93 (d, 2H, *J* = 7.6 Hz, Ph *o*-CH), 6.83 (d, 2H, *J* = 7.2 Hz, Ph *m*-CH), 6.68 (d, 2H, *J* = 7.6 Hz, *p*-tolyl *m*-CH), 6.58−6.50 (m, 3H, Ph *p*-C, Ph *o*-CH), 6.37−6.31 (m, 4H, Ph *m*-CH), 6.19 (t, 1H, *J* = 7.2 Hz, Ph *p*-CH), 6.06 (d, 2H, *J* = 8.0 Hz, Ph *o*-CH), 2.48 (s, 3H, *p*-tolyl CH_3), 2.25 (s, 3H, *p*-tolyl CH_3), 2.11 (s, 3H, *p*-tolyl CH_3).^{13}C NMR (CD_2Cl_2, 100 MHz, 25 °C): 151.2 (NCN), 149.3 (NCN), 148.9 (NCN), 148.1(Ph *i*-C), 147.7 (Ph *i*-C), 146.8 (Ph *i*-C), 146.3 (Ph *i*-C), 143.2 (Ph *i*-C), 142.8 (Ph *i*-C), 139.5 (*p*-tolyl *p*-C), 139.4 (*p*-tolyl *p*-C), 139.2 (*p*-tolyl *p*-C), 131.7, 129.8 (*p*-tolyl *m*-C), 129.3 (*p*-tolyl *m*-C), 129.3, 129.2, 129.1, 128.9, 128.8 (*p*-tolyl *m*-C), 128.4 (*p*-tolyl *o*-C), 128.4 (Ph *m*-C), 127.9 (Ph *m*-C), 127.3 (Ph *o*-C), 126.7 (*p*-tolyl *o*-C), 125.8 (*p*-tolyl *i*-C), 125.6, 125.6 (*p*-tolyl *o*-C), 125.0 (Ph *o*-C), 124.9 (Ph *o*-C), 123.5, 123.4, 122.4 (Ph *p*-C), 122.1 (Ph *o*-C), 120.6 (Ph *p*-C), 120.2 (Ph *m*-C), 21.5 (*p*-tolyl CH_3), 21.4 (*p*-tolyl CH_3), 21.3 (*p*-tolyl CH_3). ^{11}B NMR (C_6D_6, 128 MHz, 25 °C): 26.3 (fwhh = 970 Hz), 2.3 (fwhh = 220 Hz). Anal. Calcd for $C_{60}H_{51}B_3N_{12}$: C, 74.10; H, 5.29; N, 17.28. Found: C, 74.02; H, 5.36; N, 16.75.

Characterization Data for Compound 5. ^1H NMR (CD_2Cl_2, 400 MHz, 25 °C): 7.91 (d, 4H, *J* = 7.6 Hz), 7.47−7.39 (m, 6H), 7.24−7.19 (m, 6H, Ph *o*-CH), 7.15 (d, 4H, *J* = 8.0 Hz, Ph *m*-CH), 7.08 (d, 1H, *J* = 6.4 Hz), 7.01 (d, 2H, *J* = 8.4 Hz, Ph *o*-CH), 6.92−6.88 (m, 6H, Ph *o*-CH), 6.77−6.71 (m, 6H, Ph *m*-CH), 6.66 (t, 2H, *J* = 7.2 Hz), 6.65−6.60 (m, 3H), 6.57 (d, 2H, *J* = 8.4 Hz, Ph *m*-CH), 2.39 (s, 3H, *p*-tolyl CH_3), 1.80 (s, 3H, *p*-tolyl CH_3), 1.77 (s, 3H, *p*-tolyl CH_3). ^{13}C NMR (CD_2Cl_2, 100 MHz, 25 °C): 155.1, 151.5, 147.6, 146.3, 145.5, 144.1, 142.7, 142.2, 139.4, 139.2, 138.1, 131.8, 131.7, 129.6, 129.6, 129.4, 129.2, 129.0, 129.0, 128.9, 128.8, 128.7, 128.7, 128.6, 128.4, 128.3, 128.2, 128.0, 125.6, 125.1, 124.4, 124.2, 123.3, 120.9, 120.4, 116.1, 114.0 (Ph *o*-C), 21.3 (*p*-tolyl CH_3), 20.8 (*p*-tolyl CH_3), 20.8 (*p*-tolyl CH_3). ^{11}B NMR (C_6D_6, 128 MHz, 25 °C): 25.1 (fwhh = 720 Hz), −0.3 (fwhh = 122 Hz). Anal. Calcd for $C_{60}H_{51}B_3N_{12}(C_7H_8)$: C, 75.58; H, 5.59; N, 15.79. Found: C, 75.18; H, 5.59; N, 15.89.

Characterization Data for Compound 6. ^1H NMR (THF-d_8, 400 MHz, −60 °C): δ 8.15 (d, 2H, *J* = 7.6 Hz, *p*-tolyl *o*-CH), 7.91 (d, 1H, *J* = 7.2 Hz, C_6H_4), 7.79 (d, 2H, *J* = 7.6 Hz, *p*-tolyl *o*-CH), 7.50 (br, 2H, Ph), 7.41 (d, 2H, *J* = 7.6 Hz, *p*-tolyl *o*-CH), 7.20 (d, 2H, *J* = 7.6 Hz, Ph *o*-CH), 7.10 (d, 2H, *J* = 7.6 Hz, *p*-tolyl *m*-CH), 7.06 (br, 2H, Ph), 6.97 (t, 2H, *J* = 7.2 Hz, Ph *m*-CH), 6.94 (br, 1H, Ph), 6.89 (d, 1H, *J* = 7.2 Hz, Ph), 6.83 (d, 2H, *J* = 8.0 Hz, *p*-tolyl *m*-CH), 6.78 (d, 2H, *J* = 7.6 Hz, *p*-tolyl *m*-CH), 6.76−6.67 (overlapped, 3H, 2 × C_6H_4 + 1 × Ph), 6.63−6.51 (overlapped, 3H, Ph), 6.51−6.39 (overlapped, 5H, 4 × Ph + 1 × C_6H_4), 6.38−6.28 (overlapped, 2H, Ph), 6.23−6.07 (overlapped, 3H, Ph), 6.02 (t, 1H, *J* = 7.5 Hz, Ph), 5.67 (t, 1H, *J* = 7.5 Hz, Ph), 3.40 (s, 12H, O−CH_2 DME), 3.24 (s, 18H, O−CH_3 DME), 2.32 (s, 3H, *p*-tolyl), 2.20 (s, 3H, *p*-tolyl), 2.08 (s, 3H, *p*-tolyl). ^{13}C NMR (THF-d_8, 100 MHz, −60 °C): 149.6, 148.7, 148.0, 147.9, 147.7, 143.6, 143.4, 142.9, 136.9, 136.5, 135.4, 130.2, 130.2, 128.2, 128.1, 128.0, 127.7, 127.6, 127.3, 127.2, 126.8, 126.7, 126.4, 126.2, 126.1, 126.0, 125.7, 123.4, 123.2, 122.8, 122.1, 121.3, 120.5, 119.7, 119.2, 118.4, 117.5, 115.1, 112.8, 112.5, 112.0, 111.8, 109.5, 71.7 (O−CH_2 DME), 58.0 (O−CH_3 DME), 20.7 (*p*-tolyl CH_3), 20.6 (*p*-tolyl CH_3), 20.3 (*p*-tolyl CH_3). ^{11}B NMR (THF-d_8, 128 MHz, −60 °C): 28.2 (fwhh = 1420 Hz), 5.4 (fwhh = 150 Hz). Anal. Calcd for $C_{75}H_{87}B_3N_{12}NaO_6$: C, 68.87; H, 6.70; N, 12.85. Found: C, 68.13; H, 6.66; N, 12.67.

Synthesis of [Na(15-c-5)][5]. To a solution of **5** (21.5 mg, 0.020 mmol) in 1.5 mL of THF were added Na/Hg (2.447% of Na, 22.8 mg, 0.024 mmol) and 15-crown-5 (4 μL, 0.020 mmol). The mixture was stirred for 5 h, after which the supernatant solution was separated from Hg(l) using a pipet. Addition of hexane to the THF solution precipitated 24.3 mg of **5** as green crystalline material (0.019 mmol, 99%). Anal. Calcd for $C_{70}H_{71}B_3N_{12}NaO_5$: C, 69.15; H, 5.89; N, 13.82. Found: C, 69.09; H, 5.90; N, 13.59.

Reactions of 3−5 with XeF_2. A solution was prepared of ca. 5 mg of **3**, **4**, or **5** in 0.45 mL of C_6D_6 that contained C_6F_6 as an internal standard. The required amount of XeF_2 (see main text) was added as a solid. Upon dissolution of the XeF_2, the reactions were monitored by ^1H and ^{19}F NMR spectroscopy. Yields of compound **1** were determined by integration of the ^{19}F NMR signal of the BF_2 moiety in **1** (δ −144 ppm) relative to the C_6F_6 internal standard. NMR spectra of these reactions are provided in the Supporting Information.

■ ASSOCIATED CONTENT

Supporting Information

The Supporting Information is available free of charge on the ACS Publications website at DOI: 10.1021/acs.inorgchem.5b01287.

Cyclic voltammogram for **3**, details of X-ray structure determination of $[Na(THF)_3]^+[\mathbf{3}]^{\bullet-}$ and $[Na(15\text{-}c\text{-}5)]^+[\mathbf{5}]^{\bullet-}$, NMR spectral data, DFT calculated energies, and coordinates for the DFT optimized geometries (PDF)

X-ray crystallographic data files for **3**−**6**, $[Na(THF)_3]^+[\mathbf{3}]^{\bullet-}$, and $[Na(15\text{-}c\text{-}5)]^+[\mathbf{5}]^{\bullet-}$ (CIF)

■ AUTHOR INFORMATION

Corresponding Author

*E-mail: edwin.otten@rug.nl.

Notes

The authors declare no competing financial interest.

■ ACKNOWLEDGMENTS

Financial support from the Netherlands Organisation for Scientific Research (NWO) is gratefully acknowledged (Veni grant to E.O.). We thank Prof. W. R. Browne (University of Groningen) for the use of spectroscopic facilities and help with quantum yield determination.

■ REFERENCES

(1) (a) Bourissou, D.; Guerret, O.; Gabbaï, F. P.; Bertrand, G. *Chem. Rev.* **2000**, *100*, 39. (b) Hahn, F. E.; Jahnke, M. C. *Angew. Chem., Int. Ed.* **2008**, *47*, 3122. (c) Hopkinson, M. N.; Richter, C.; Schedler, M.; Glorius, F. *Nature* **2014**, *510*, 485.

(2) (a) Mizuhata, Y.; Sasamori, T.; Tokitoh, N. *Chem. Rev.* **2009**, *109*, 3479. (b) Blom, B.; Stoelzel, M.; Driess, M. *Chem. - Eur. J.* **2013**, *19*, 40. (c) Blom, B.; Gallego, D.; Driess, M. *Inorg. Chem. Front.* **2014**, *1*, 134.

(3) Fischer, R. C.; Power, P. P. *Chem. Rev.* **2010**, *110*, 3877.

(4) (a) Vidovic, D.; Pierce, G. A.; Aldridge, S. *Chem. Commun.* **2009**, 1157. (b) Vidovic, D.; Aldridge, S. *Chem. Sci.* **2011**, *2*, 601. (c) Brand, J.; Braunschweig, H.; Sen, S. S. *Acc. Chem. Res.* **2014**, *47*, 180. (d) Braunschweig, H.; Dewhurst, R. D.; Gessner, V. H. *Chem. Soc. Rev.* **2013**, *42*, 3197.

(5) Timms, P. L. *Acc. Chem. Res.* **1973**, *6*, 118.

DOI: 10.1021/acs.inorgchem.5b01287
Inorg. Chem. 2015, 54, 8656−8664

(6) van der Kerk, S. M.; Boersma, J.; van der Kerk, G. J. M. *Tetrahedron Lett.* **1976**, *17*, 4765.
(7) (a) Ramsey, B. G.; Anjo, D. M. *J. Am. Chem. Soc.* **1977**, *99*, 3182. (b) Pachaly, B.; West, R. *Angew. Chem., Int. Ed. Engl.* **1984**, *23*, 454.
(8) Bettinger, H. F. *J. Am. Chem. Soc.* **2006**, *128*, 2534.
(9) Krasowska, M.; Bettinger, H. F. *J. Am. Chem. Soc.* **2012**, *134*, 17094.
(10) (a) Wang, Y.; Quillian, B.; Wei, P.; Wannere, C. S.; Xie, Y.; King, R. B.; Schaefer, H. F.; Schleyer, P. v. R.; Robinson, G. H. *J. Am. Chem. Soc.* **2007**, *129*, 12412. (b) Wang, Y.; Quillian, B.; Wei, P.; Xie, Y.; Wannere, C. S.; King, R. B.; Schaefer, H. F.; Schleyer, P. v. R.; Robinson, G. H. *J. Am. Chem. Soc.* **2008**, *130*, 3298. (c) Bissinger, P.; Braunschweig, H.; Damme, A.; Kupfer, T.; Vargas, A. *Angew. Chem., Int. Ed.* **2012**, *51*, 9931.
(11) (a) Braunschweig, H.; Dewhurst, R. D.; Hammond, K.; Mies, J.; Radacki, K.; Vargas, A. *Science* **2012**, *336*, 1420. (b) Koppe, R.; Schnockel, H. *Chem. Sci.* **2015**, *6*, 1199. (c) Böhnke, J.; Braunschweig, H.; Constantinidis, P.; Dellermann, T.; Ewing, W. C.; Fischer, I.; Hammond, K.; Hupp, F.; Mies, J.; Schmitt, H.-C.; Vargas, A. *J. Am. Chem. Soc.* **2015**, *137*, 1766.
(12) (a) Bissinger, P.; Braunschweig, H.; Damme, A.; Dewhurst, R. D.; Kupfer, T.; Radacki, K.; Wagner, K. *J. Am. Chem. Soc.* **2011**, *133*, 19044. (b) Bissinger, P.; Braunschweig, H.; Kraft, K.; Kupfer, T. *Angew. Chem., Int. Ed.* **2011**, *50*, 4704. (c) Curran, D. P.; Boussonnière, A.; Geib, S. J.; Lacôte, E. *Angew. Chem., Int. Ed.* **2012**, *51*, 1602.
(13) (a) Kinjo, R.; Donnadieu, B.; Celik, M. A.; Frenking, G.; Bertrand, G. *Science* **2011**, *333*, 610. (b) Kong, L.; Li, Y.; Ganguly, R.; Vidovic, D.; Kinjo, R. *Angew. Chem., Int. Ed.* **2014**, *53*, 9280. (c) Dahcheh, F.; Martin, D.; Stephan, D. W.; Bertrand, G. *Angew. Chem., Int. Ed.* **2014**, *53*, 13159.
(14) Segawa, Y.; Yamashita, M.; Nozaki, K. *Science* **2006**, *314*, 113.
(15) Asay, M.; Jones, C.; Driess, M. *Chem. Rev.* **2011**, *111*, 354.
(16) (a) Reiher, M.; Sundermann, A. *Eur. J. Inorg. Chem.* **2002**, *2002*, 1854. (b) Chen, C.-H.; Tsai, M.-L.; Su, M.-D. *Organometallics* **2006**, *25*, 2766.
(17) Firinci, E.; Bates, J. I.; Riddlestone, I. M.; Phillips, N.; Aldridge, S. *Chem. Commun.* **2013**, *49*, 1509.
(18) For selected reviews on the chemistry of redox-active ligands, see: (a) Chirik, P. J.; Wieghardt, K. *Science* **2010**, *327*, 794. (b) Lyaskovskyy, V.; de Bruin, B. *ACS Catal.* **2012**, *2*, 270. (c) Praneeth, V. K. K.; Ringenberg, M. R.; Ward, T. R. *Angew. Chem., Int. Ed.* **2012**, *51*, 10228. (d) Luca, O. R.; Crabtree, R. H. *Chem. Soc. Rev.* **2013**, *42*, 1440.
(19) Sigeikin, G. I.; Lipunova, G. N.; Pervova, I. G. *Russ. Chem. Rev.* **2006**, *75*, 885.
(20) (a) Gilroy, J. B.; Ferguson, M. J.; McDonald, R.; Patrick, B. O.; Hicks, R. G. *Chem. Commun.* **2007**, 126. (b) Chang, M. C.; Otten, E. *Chem. Commun.* **2014**, *50*, 7431. (c) Barbon, S. M.; Reinkeluers, P. A.; Price, J. T.; Staroverov, V. N.; Gilroy, J. B. *Chem. - Eur. J.* **2014**, *20*, 11340. (d) Barbon, S. M.; Price, J. T.; Reinkeluers, P. A.; Gilroy, J. B. *Inorg. Chem.* **2014**, *53*, 10585. (e) Hesari, M.; Barbon, S. M.; Staroverov, V. N.; Ding, Z.; Gilroy, J. B. *Chem. Commun.* **2015**, *51*, 3766.
(21) (a) Chang, M.-C.; Dann, T.; Day, D. P.; Lutz, M.; Wildgoose, G. G.; Otten, E. *Angew. Chem., Int. Ed.* **2014**, *53*, 4118. (b) Chang, M.-C.; Roewen, P.; Travieso-Puente, R.; Lutz, M.; Otten, E. *Inorg. Chem.* **2015**, *54*, 379. (c) Travieso-Puente, R.; Chang, M.-C.; Otten, E. *Dalton Trans.* **2014**, *43*, 18035. (d) Zaidman, A. V.; Pervova, I. G.; Vilms, A. I.; Belov, G. P.; Kayumov, R. R.; Slepukhin, P. A.; Lipunov, I. N. *Inorg. Chim. Acta* **2011**, *367*, 29. (e) Hong, S.; Hill, L. M. R.; Gupta, A. K.; Naab, B. D.; Gilroy, J. B.; Hicks, R. G.; Cramer, C. J.; Tolman, W. B. *Inorg. Chem.* **2009**, *48*, 4514. (f) Gilroy, J. B.; Ferguson, M. J.; McDonald, R.; Hicks, R. G. *Inorg. Chim. Acta* **2008**, *361*, 3388. (g) Gilroy, J. B.; Patrick, B. O.; McDonald, R.; Hicks, R. G. *Inorg. Chem.* **2008**, *47*, 1287. (h) Tezcan, H.; Uzluk, E.; Aksu, M. L. *Electrochim. Acta* **2008**, *53*, 5597.
(22) *CRC Handbook of Chemistry and Physics*, 96 ed.; CRC Press: Boca Raton, FL, 2015−2016.
(23) Rablen, P. R.; Hartwig, J. F. *J. Am. Chem. Soc.* **1996**, *118*, 4648.
(24) Connelly, N. G.; Geiger, W. E. *Chem. Rev.* **1996**, *96*, 877.
(25) (a) Bai, G.; Wei, P.; Stephan, D. W. *Organometallics* **2006**, *25*, 2649. (b) Basuli, F.; Kilgore, U. J.; Brown, D.; Huffman, J. C.; Mindiola, D. J. *Organometallics* **2004**, *23*, 6166. (c) Obenhuber, A. H.; Gianetti, T. L.; Berrebi, X.; Bergman, R. G.; Arnold, J. *J. Am. Chem. Soc.* **2014**, *136*, 2994.
(26) (a) Cramer, C. J.; Tolman, W. B. *Acc. Chem. Res.* **2007**, *40*, 601. (b) Yamashita, M.; Aramaki, Y.; Nozaki, K. *New J. Chem.* **2010**, *34*, 1774. (c) Li, J.; Li, X.; Huang, W.; Hu, H.; Zhang, J.; Cui, C. *Chem. - Eur. J.* **2012**, *18*, 15263. (d) Xie, L.; Zhang, J.; Hu, H.; Cui, C. *Organometallics* **2013**, *32*, 6875.
(27) (a) Bowman, W. R.; Storey, J. M. D. *Chem. Soc. Rev.* **2007**, *36*, 1803. (b) Studer, A.; Bossart, M. In *Radicals in Organic Synthesis*; Renaud, P., Sibi, M. P., Eds.; Wiley-VCH Verlag GmbH: Weinheim, Germany, 2008; Vol. 2, p 62. (c) Beaume, A.; Courillon, C.; Derat, E.; Malacria, M. *Chem. - Eur. J.* **2008**, *14*, 1238.
(28) (a) Boese, R.; Maulitz, A. H.; Stellberg, P. *Chem. Ber.* **1994**, *127*, 1887. (b) Kiran, B.; Phukan, A. K.; Jemmis, E. D. *Inorg. Chem.* **2001**, *40*, 3615. (c) Anand, B.; Nöth, H.; Schwenk-Kircher, H.; Troll, A. *Eur. J. Inorg. Chem.* **2008**, *2008*, 3186.
(29) Lisovenko, A. S.; Timoshkin, A. Y. *Inorg. Chem.* **2010**, *49*, 10357.
(30) Buemi, G.; Zuccarello, F.; Venuvanalingam, P.; Ramalingam, M.; Salai Cheettu Ammal, S. *J. Chem. Soc., Faraday Trans.* **1998**, *94*, 3313.
(31) (a) Findlater, M.; Hill, N. J.; Cowley, A. H. *Dalton Trans.* **2008**, 4419. (b) Aramaki, Y.; Omiya, H.; Yamashita, M.; Nakabayashi, K.; Ohkoshi, S.-i.; Nozaki, K. *J. Am. Chem. Soc.* **2012**, *134*, 19989.
(32) Frisch, M. J.; Trucks, G. W.; Schlegel, H. B.; Scuseria, G. E.; Robb, M. A.; Cheeseman, J. R.; Scalmani, G.; Barone, V.; Mennucci, B.; Petersson, G. A.; Nakatsuji, H.; Caricato, M.; Li, X.; Hratchian, H. P.; Izmaylov, A. F.; Bloino, J.; Zheng, G.; Sonnenberg, J. L.; Hada, M.; Ehara, M.; Toyota, K.; Fukuda, R.; Hasegawa, J.; Ishida, M.; Nakajima, T.; Honda, Y.; Kitao, O.; Nakai, H.; Vreven, T.; Montgomery, J. A., Jr.; Peralta, J. E.; Ogliaro, F.; Bearpark, M. J.; Heyd, J.; Brothers, E. N.; Kudin, K. N.; Staroverov, V. N.; Kobayashi, R.; Normand, J.; Raghavachari, K.; Rendell, A. P.; Burant, J. C.; Iyengar, S. S.; Tomasi, J.; Cossi, M.; Rega, N.; Millam, N. J.; Klene, M.; Knox, J. E.; Cross, J. B.; Bakken, V.; Adamo, C.; Jaramillo, J.; Gomperts, R.; Stratmann, R. E.; Yazyev, O.; Austin, A. J.; Cammi, R.; Pomelli, C.; Ochterski, J. W.; Martin, R. L.; Morokuma, K.; Zakrzewski, V. G.; Voth, G. A.; Salvador, P.; Dannenberg, J. J.; Dapprich, S.; Daniels, A. D.; Farkas, Ö.; Foresman, J. B.; Ortiz, J. V.; Cioslowski, J.; Fox, D. J. *Gaussian 09*, Revision C.01; Gaussian, Inc.: Wallingford, CT,2009.
(33) *APEX2* (v2012.4-3), *SAINT* (Version 8.18C), and *SADABS* (Version 2012/1); Bruker AXS Inc.: Madison, WI, 2012.
(34) Sheldrick, G. *Acta Crystallogr., Sect. A: Found. Crystallogr.* **2008**, *64*, 112.

DOI: 10.1021/acs.inorgchem.5b01287
Inorg. Chem. 2015, 54, 8656−8664